American Mineralogist, Volume 81, pages 1092–1096, 1996

High-pressure, high-temperature Raman spectroscopic study of ilmenite-type $MgSiO_3$

BRUNO REYNARD[1] AND DAVID C. RUBIE[2]

[1]Laboratoire de Minéralogie Physique, Géosciences Rennes, CNRS-UPR 4661, Institut de Géologie, Université de Rennes I 35042 Rennes Cedex, France
[2]Bayerisches Geoinstitut, Universität Bayreuth, D-95440 Bayreuth, Germany

ABSTRACT

High-pressure and high-temperature Raman spectra of ilmenite-type $MgSiO_3$ have been collected up to 7 GPa and 1030 K, respectively. The observed Raman frequency shifts with pressure and temperature were used to calculate the isothermal, isobaric, and isochoric (or intrinsic) anharmonic mode parameters. The low values of the intrinsic mode parameters indicate that ilmenite-type $MgSiO_3$ has a nearly quasi-harmonic behavior, and intrinsic anharmonic corrections to the entropy and relative enthalpy of ilmenite-type $MgSiO_3$ do not exceed 4(3) J/(mol·K) and 4(3) kJ/mol at 2000 K, respectively. These corrections are lower than those inferred for other mantle minerals. Above 900 K, a back-transformation to an $MgSiO_3$ glass was first observed, prior to recrystallization to enstatite near 1000 K. Back-transformation systematics for high-pressure silicate phases are discussed.

INTRODUCTION

Ilmenite-type $MgSiO_3$ is a high-pressure polymorph of enstatite that is characterized by a relatively narrow stability field (Ito and Matsui 1977; Ito and Yamada 1982; Ito and Navrotsky 1985; Sawamoto 1987) in the 20–24 GPa range, bounded at lower pressures by the β-Mg_2SiO_4 + stishovite assemblage stability field, at higher pressures and temperatures by the perovskite-type $MgSiO_3$ stability field, and, marginally, at high temperatures (>2200 K) by the majorite stability field. Its stability at relatively low temperatures makes it a candidate mantle-forming phase in subducting slabs in the 600–700 km depth range. A detailed knowledge of its stability is important for understanding the dynamics of subducted slabs and for refining thermodynamic databases for phase-diagram calculations. In the thermodynamic modeling of the high-pressure phase relations in the MgO-SiO_2 system (e.g., Ashida et al. 1988; Fei et al. 1990), vibrational models are commonly used to extrapolate the low-temperature thermochemical data obtained from high-pressure phases to the temperature conditions pertinent to the Earth's mantle. These models always assume the quasi-harmonic approximation, hence the Dulong and Petit limit for the heat capacity at high temperature. Combined calorimetric and vibrational studies of olivines have shown that this approximation fails at high temperature because of the occurrence of intrinsic anharmonic effects (Gillet et al. 1991; Fiquet et al. 1992). These effects can be included in vibrational modeling provided that high-temperature, high-pressure Raman spectroscopic data are available. An evaluation of intrinsic anharmonic effects in high-pressure phases is thus needed to refine the vibrational modeling of their high-temperature thermochemical properties. In their study of geikielite (ilmenite-type $MgTiO_3$), Reynard and Guyot (1994) suggested that these effects may be negligible for the ilmenite structure, whereas they are important in the garnet structure (Gillet et al. 1992). This would lead to significant intrinsic anharmonic corrections to the entropy and enthalpy changes associated with the ilmenite-majorite transformation. Thus, we conducted a high-pressure, high-temperature Raman spectroscopic study of high-pressure silicates and present here the results obtained for ilmenite-type $MgSiO_3$.

EXPERIMENTAL METHODS

Sample synthesis

Powder of dry $MgSiO_3$ glass synthesized by Neuville and Richet (1991) was used as a starting material and transformed at 22 GPa and 1200 °C for 2.5 h using the 1200 ton multi-anvil press at the Bayerisches Geoinstitut. It was confirmed by both X-ray powder diffraction and Raman spectroscopy that the sample consisted of pure ilmenite phase. Least-squares refinement of the ambient lattice parameters from the X-ray diffraction data gave $a = 4.722(2)$ and $c = 13.560(12)$ Å, in good agreement with previous determinations (Ito and Matsui 1977). Grain size is about 5–10 μm (optical observation).

High-pressure, high-temperature Raman spectroscopy

Raman spectra were collected using a DILOR XY double substractive microspectrometer equipped with 1200 g/mm gratings and an ORTEC CCD nitrogen-cooled detector at the University of Rennes. The 488 or 514.5 nm line of a Spectra Physic Ar laser was used to excite the Raman scattering and ruby fluorescence.

For the high-pressure experiments, a diamond-anvil cell

0003–004X/96/0910–1092$05.00

was used. The sample was placed in the 200 μm diameter hole of an Inconel gasket along with H_2O as the pressure medium and ruby chips (~5 μm) for pressure measurements. Anvil culets measured 700 μm. No measurable pressure gradients were detected up to the maximum pressure reached in this study (7 GPa). H_2O was preferred to an alcohol mixture because it has no strong Raman band that may interfere with the weak Raman signal from the sample. The Ar laser light was focused onto the sample or ruby through a Leitz UTK 40 objective with a working distance of 14 mm and numerical aperture of 0.32. The Raman light was collected in the backscattering geometry through the same objective and focused in the spectrometer through a 100 μm slit defining a spectral resolution of about 10 μm, giving a bandpass of about 2.5 cm^{-1}.

High-temperature experiments were performed using a Leitz 1350 heating stage. Temperature was monitored with a Pt-PtRh10 thermocouple calibrated against known melting-point compounds. Temperature measurements are accurate to within a few kelvins. An Olympus ULWD 50 objective (working distance 8 mm, numerical aperture 0.63) and a slit width of 60 μm were used.

Results and discussion

High-pressure, high-temperature Raman spectra

The ambient-condition Raman spectrum of ilmenite-type $MgSiO_3$ gives nine observable bands at 294, 351, 402, 413, 484, 499, 620, 680, and 798 cm^{-1} out of the ten expected from symmetry analysis (five A_g and five E_g), in agreement within a few wavenumbers with previous determinations by McMillan and Ross (1987). Although several spectra were recorded on different grains, the tenth expected band was not observed.

It was noticed that heating due to the laser could perturb the Raman experiment. This is illustrated in Figure 1, where the evolution of the frequency and line width of the 798 cm^{-1} band with increasing laser power is compared to its evolution with increasing temperature in the high-temperature cell. This evolution (Fig. 1) for a laser output power of 2 W (maximum power on the 514.53 nm line of the Ar laser) is equivalent to that from heating to 200 °C, and the heating effect is nearly linear with the output power down to 100 mW. An output power of 200 mW, which gives a heating effect estimated to be <50 K, was chosen as a compromise to keep the recording times within reasonable limits of about 10 min at high temperature. For the high-pressure experiments, the laser power was 500 mW because the effective power at the sample is lower owing to the different objective used and the absorption by the diamond window.

The overall intensity of the Raman bands was very low and decreased dramatically with pressure, which impeded recording of the spectra above 7 GPa. However, the nine bands could be followed up to this pressure, and no transformation or hysteresis upon decompression was observed. The Raman frequency shifts with pressure ob-

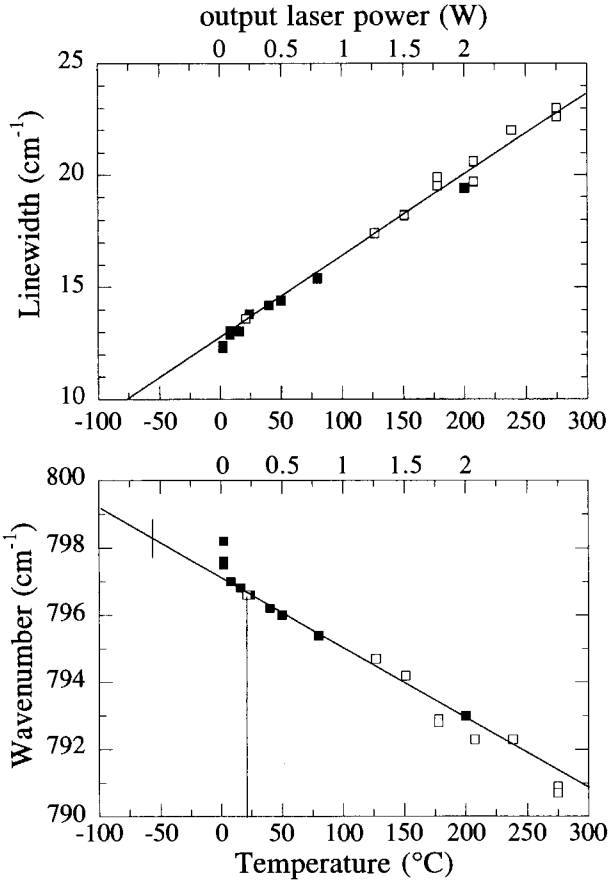

Figure 1. Estimation of the heating effect of the argon laser. Solid symbols represent the evolution of the line width (**top**) and frequency (**bottom**) of the intense 798 cm^{-1} mode with increasing laser power (top scale) out of the heating stage. Open symbols are the data obtained for the same mode at high temperatures (bottom scale) for a constant laser output power of 200 mW.

tained from a linear regression of the high-pressure data (Fig. 2a) are reported in Table 1. These data complement those obtained by Liu et al. (1994).

At high temperature no transformation was observed up to 880 K, and the frequency shifts and line-width increase with temperature could be determined for the nine bands observed at ambient conditions (Figs. 2b and 3). Frequencies and line widths were obtained by deconvolution of the high-temperature spectra using Voigt-type profiles for the Raman bands. The frequency vs. temperature relations are curved for most bands, with the exception of the 798 and 680 cm^{-1} bands, which do not depart significantly from a straight line. Curves were fitted using the relationship (Reynard and Guyot 1994)

$$\nu = A + BT + C/[T + (C/B)^{1/2}] \quad (1)$$

in which A, B, and C are adjustable parameters. This expression fixes the value of the slope $(\partial\nu/\partial T)_P$ to zero at 0 K and to B at infinite temperature, as expected for a quasi-harmonic oscillator (e.g., Maradudin and Fein

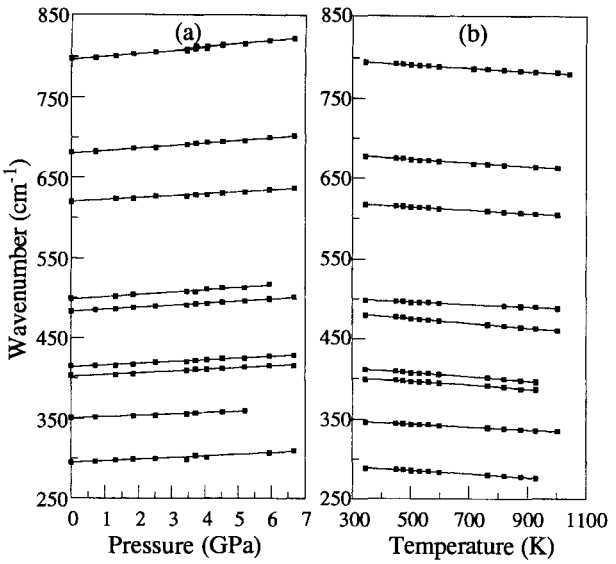

FIGURE 2. Evolution of Raman frequencies with (**a**) pressure and (**b**) temperature. For the high-temperature data, the points above 900 K were not included in the fit because of the onset of back-transformation.

1962). It is preferred to a second-order polynomial, which has the same number of adjustable parameters, because it gives a realistic extrapolation toward low temperatures. This is important to constrain the ambient-temperature slope, which is used to calculate the anharmonic parameters (see below), in the absence of data below 300 K. Although this expression is derived for a quasi-harmonic oscillator, the actual value of the slope at ambient temperature obtained from the fit is constrained by the measured frequencies at high temperature and can account for deviations from the quasi-harmonic behavior (intrinsic anharmonicity). The slopes at ambient temperature are reported in Table 1.

Above 880 K, the onset of a partial transformation of ilmenite-type $MgSiO_3$ to a glass is observed, marked by the appearance of broad bands in the 850–1050 cm^{-1} range. Upon increasing temperature, this transformation is enhanced and the glass finally starts to recrystallize to enstatite near 1000 K. The relative amounts of vitrified and recrystallized low-pressure phases, and of preserved ilmenite, vary within the samples quenched from 1030 K (Fig. 3).

Mode anharmonic parameters and intrinsic anharmonicity

From the observed frequency shifts with pressure and temperature, the isothermal Grüneisen (γ_{iT}) and isobaric anharmonic (γ_{iP}) mode parameters can be calculated as (Grüneisen 1912; Gillet et al. 1989)

$$\gamma_{iT} = K_T(\partial \ln \nu_i/\partial P)_T \quad (2)$$

$$\gamma_{iP} = 1/\alpha(\partial \ln \nu_i/\partial T)_P \quad (3)$$

TABLE 1. High-pressure and high-temperature frequency shifts of ilmenite-type $MgSiO_3$ and mode anharmonic parameters

ν_i (cm^{-1})	$(\partial\nu_i/\partial P)_T$ (cm^{-1}·GPa^{-1})	γ_{iT}	$(\partial\nu_i/\partial T)_{P,298\,K}$ (cm^{-1}·K^{-1})	γ_{iP}	a_i (10^{-5} K^{-1})
294	2.1(2)	1.6(2)	−0.0203(16)	2.3(4)	−1.7(15)
351	1.7(1)	1.1(1)	−0.0174(17)	2.0(4)	−2.3(12)
402	2.2(1)	1.24(6)	−0.024(3)	1.3(3)	−0.1(9)
413	2.3(1)	1.26(6)	−0.027(3)	1.8(4)	−1.2(10)
484	2.65(7)	1.24(4)	−0.0285(19)	2.3(4)	−2.6(10)
499	3.1(2)	1.40(3)	−0.0148(16)	1.05(20)	0.9(6)
620	2.4(1)	0.88(2)	−0.0192(11)	1.16(18)	−0.7(5)
680	3.3(1)	1.10(2)	−0.0245(5)	1.38(16)	−0.7(5)
798	3.7(1)	1.04(2)	−0.0212(5)	1.07(13)	−0.1(4)

where ν_i is the vibrational frequency of the ith mode, K_T is the isothermal bulk modulus, and α is the thermal expansivity. We used the mean value of α of 2.44 × 10^{-5} K^{-1} determined in the 295–876 K temperature range by Ashida et al. (1988) and a value of K_T of 212 GPa, similar to that inferred for K_S by Weidner and Ito (1985) and consistent with the static compression experiment by Reynard et al. (1996a). Values of γ_{iT} and γ_{iP} are reported in Table 1. The average Grüneisen parameter $\langle\gamma\rangle$ is given by

$$\langle\gamma\rangle = \Sigma\, \gamma_{iT}C_{Vi}/\Sigma\, C_{Vi} \quad (4)$$

and yields a value of 1.38 at 298 K and 1.24 in the high-temperature limit. The values of the isothermal and isobaric anharmonic parameters can be used to obtain the intrinsic anharmonic mode parameters a_i (Mammone and Sharma 1979; Gillet et al. 1989):

$$\begin{aligned} a_i &= (\partial \ln \nu_i/\partial T)_V \\ &= \alpha K_T(\partial \ln \nu_i/\partial P)_T - (\partial \ln \nu_i/\partial T)_P \\ &= \alpha(\gamma_{iT} - \gamma_{iP}). \end{aligned} \quad (5)$$

The values of a_i are reported in Table 1. Their absolute values are low and not significantly different from zero for six modes. For the three other modes, the values are significantly negative. This is consistent with the results obtained for geikielite (Reynard and Guyot 1994). The mean intrinsic anharmonic parameter $\bar{a}$ is −0.9(7) × 10^{-5} K^{-1}, which gives very low estimates of the anharmonic correction for the heat capacity ($\approx -6n\bar{a}RT$, where n is the number of atoms per formula unit), entropy S ($\approx -6n\bar{a}RT$), and relative enthalpy ΔH ($\approx -3n\bar{a}RT^2$) (Gillet et al. 1991; Reynard et al. 1996b) of 4(3) J/(mol·K), 4(3) J/(mol·K), and 4(3) kJ/mol at 2000 K, respectively. Thus, the intrinsic anharmonic corrections to the thermochemical properties of ilmenite are probably insignificant. Following Reynard and Guyot (1994), we can assume that the mean intrinsic anharmonic parameter for majorite is similar to that obtained for garnets by Gillet et al. (1992) of 2 × 10^{-5} K^{-1}, i.e., higher than that of the ilmenite-type structure. Using these values, the anharmonic contributions to the ΔH and ΔS of the ilmenite-majorite transition at various temperatures can be ob-

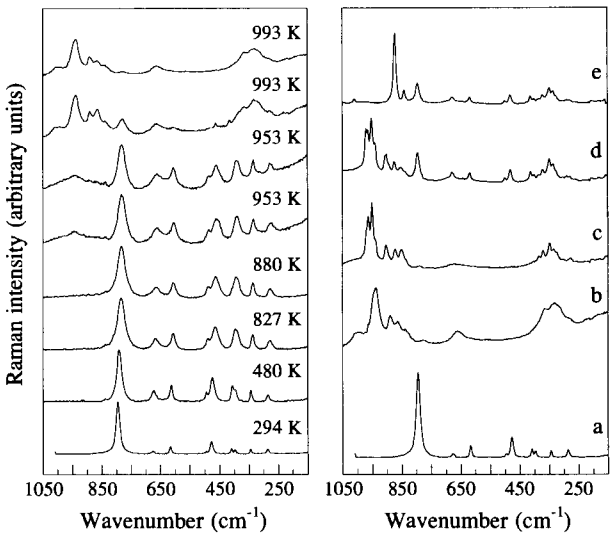

FIGURE 3. (**left**) Evolution of the Raman spectra with temperature. At 880 K, no transformation is observed; at 953 K, the partial back-transformation is marked by the appearance of a broad band near 850–1050 cm^{-1}; at 993 K, pyroxene bands appear. (**right**) (a) Spectrum of the starting material at 298 K; (b) at 993 K; (c, d, and e) spectra of different areas of the sample quenched from 1030 K showing the heterogeneous back-transformation to pyroxene and glass, marked by the different relative intensities of the ilmenite and pyroxene, and glass bands.

tained using the above expression. The effects of intrinsic anharmonicity on the position of the ilmenite + majorite equilibrium can then be estimated using the thermodynamic database of Fei et al. (1990) and correcting the enthalpies and entropies for the anharmonic contributions. At 20 GPa, these contributions reduce the calculated temperature for the transition by 200–300 K. Of course, this simple calculation provides only a rough estimate of the anharmonic effects, and a new refinement of the thermodynamic database taking into account available thermodynamic and phase-equilibrium data should be performed. High-pressure and high-temperature Raman spectroscopic studies of other phases relevant to the MgO-SiO_2 system are needed to estimate more precisely the anharmonic corrections to their thermodynamic properties.

High-temperature back-transformation

Ito and Navrotsky (1985) reported a complex decomposition of an ilmenite sample heated at 973 K for 1 h. In the recovered sample, they observed a mixture of glass and various crystalline phases, including pyroxene, and an assemblage called X, which they interpreted as a "disordered" hcp phase. In our Raman spectra at 950 K (Fig. 3), we observed the onset of the decomposition of ilmenite to a glassy phase within 10 min. The spectrum of this glassy phase is similar to that of the $MgSiO_3$ glass used as starting material. Onto these broad features are superimposed the nine bands of the ilmenite phase. At temperatures close to 1000 K, pyroxene bands appear and grow in intensity with increasing time, but the strongest band of the ilmenite phase can still be discerned. The amount of transformation varies within the quenched sample, and a mixture of the glass, ilmenite, and enstatite phases is generally observed. The ilmenite bands do not differ from those of the original sample (same frequencies and line widths). Thus, it seems that the decomposition observed here is simpler than that reported by Ito and Navrotsky (1985) and similar to that reported for perovskite-type $MgSiO_3$ by Durben and Wolf (1992), i.e., a transformation to a glass prior to a recrystallization of the glass into enstatite. A similar "amorphization" of a high-pressure phase at ambient pressure and high temperature was observed in stishovite by Gillet et al. (1990); this transformation mirrors the transformations observed during compression of quartz or its GeO_2 analog, i.e., amorphization (Hemley et al. 1988; Wolf et al. 1992). On the other hand, no amorphous phase is observed in the high-temperature back-transformation of β-Mg_2SiO_4 and γ-Ni_2SiO_4 (Yamanaka 1986; Tsukimura et al. 1988; McMillan et al. 1991; Reynard et al. 1996b). In that case, a two-step mechanism involving spinelloids is inferred (Reynard et al. 1996b), similar to the structural modifications observed in the low-pressure olivine polymorphs at high pressure and ambient temperature (Reynard et al. 1994; Andrault et al. 1995). From all these observations, it seems that metastable high-pressure phases undergo, at ambient pressure and moderate temperature, a back-transformation sequence that finds its counterpart in the structural modifications of their low-pressure polymorphs (olivines, quartz) brought out of their stability fields at high pressure and ambient temperature. Given the sluggish kinetics associated with these transformations, these observations could provide some insights into the transformation mechanisms among the different polymorphs.

REFERENCES CITED

Andrault, D., Bouhifd, M.A., Itié, J.P., and Richet, P. (1995) Compression and amorphization of $(Mg,Fe)_2SiO_4$ olivines: An X-ray diffraction study up to 70 GPa. Physics and Chemistry of Minerals, 22, 99–107.

Ashida, T., Kume, S., Ito, E., and Navrotsky, A. (1988) $MgSiO_3$ ilmenite: Heat capacity, thermal expansivity, and enthalpy of transformation. Physics and Chemistry of Minerals, 16, 239–245.

Durben, D.J., and Wolf, G.H. (1992) High-temperature behavior of metastable $MgSiO_3$ perovskite: A Raman spectroscopic study. American Mineralogist, 77, 890–893.

Fei, Y., Saxena, S.K., and Navrotsky, A. (1990) Internally consistent thermodynamic data and equilibrium phase relations for compounds in the system MgO-SiO_2 at high pressure and high temperature. Journal of Geophysical Research, 95, 6915–6928.

Fiquet, G., Gillet, P., and Richet, P. (1992) Anharmonic contributions to the heat capacity of minerals at high-temperatures. Application to Mg_2GeO_4, Ca_2GeO_4, $MgCaGeO_4$. Physics and Chemistry of Minerals, 18, 469–479.

Gillet, P., Guyot, F., and Malézieux, J.M. (1989) High-pressure and high-temperature Raman spectroscopy of Ca_2GeO_4: Some insights on anharmonicity. Physics of the Earth and Planetary Interiors, 58, 141–154.

Gillet, P., Le Cléach, A., and Madon, M. (1990) High-temperature Raman

spectroscopy of the SiO_2 and GeO_2 polymorphs: Anharmonicity and thermodynamic properties at high-temperature. Journal of Geophysical Research, 95, 21635–21655.

Gillet, P., Richet, P., Guyot, F., and Fiquet, G. (1991) High-temperature thermodynamic properties of forsterite. Journal of Geophysical Research, 96, 11805–11816.

Gillet, P., Fiquet, G., Malézieux, J.M., and Geiger, C. (1992) High-pressure and high-temperature Raman spectroscopy of end-member garnets: Pyrope, grossular and andradite. European Journal of Mineralogy, 4, 651–664.

Grüneisen, E. (1912) Theorie des festen Zustandes einatomiger Elemente. Annal Physik, 39, 257–306.

Hemley, J.R., Mao, H.K., Ming, L.C., and Manghnani, M.H. (1988) Pressure-induced amorphization of crystalline silica. Nature, 334, 52–54.

Ito, E., and Matsui, Y. (1977) Silicate ilmenites and the post-spinel transformations. In M.H. Manghnani and S. Akimoto, Eds., High pressure research: Applications to geophysics, p. 193–208. Academic, New York.

Ito, E., and Yamada, H. (1982) Stability relations of silicate spinels ilmenites and perovskites. In S. Akimoto and M.H. Manghnani, Eds., High pressure research in geophysics, p. 405–419. Center for Academic Publishing of Japan, Tokyo.

Ito, E., and Navrotsky, A. (1985) $MgSiO_3$ ilmenite: Calorimetry, phase equilibria, and decomposition at atmospheric pressure. American Mineralogist, 70, 1020–1026.

Liu, L., Mernagh, T.P., and Irifune, T. (1994) High pressure Raman spectra of β-Mg_2SiO_4, γ-Mg_2SiO_4, $MgSiO_3$-ilmenite, and $MgSiO_3$-perovskite. Journal of Physics and Chemistry of Solids, 55, 185–193.

Mammone, J.F., and Sharma, S.K. (1979) Pressure and temperature dependence of the Raman spectra of rutile-structure oxides. Carnegie Institution of Washington Year Book, 78, 369–373.

Maradudin, A.A., and Fein, A.E. (1962) Scattering of neutrons by an anharmonic crystal. Physical Review, 128, 2589–2608.

McMillan, P.F., and Ross, N.L. (1987) Heat capacity calculations for Al_2O_3 corundum and $MgSiO_3$ ilmenite. Physics and Chemistry of Minerals, 16, 225–234.

McMillan, P.F., Akaogi, M., Sato, R.K., Poe, B., and Foley, J. (1991) Hydroxyl groups in β-Mg_2SiO_4. American Mineralogist, 76, 354–360.

Neuville, D.R., and Richet, P. (1991) Viscosity and mixing in molten (Ca,Mg) pyroxenes and garnets. Geochimica et Cosmochimica Acta, 55, 1011–1019.

Reynard, B., and Guyot, F. (1994) High temperature properties of geikielite ($MgTiO_3$-ilmenite) from high-temperature high-pressure Raman spectroscopy: Some implications for $MgSiO_3$-ilmenite. Physics and Chemistry of Minerals, 21, 441–450.

Reynard, B., Petit, P.E., Guyot, F., and Gillet, P. (1994) Pressure-induced structural modifications in Mg_2GeO_4-olivine: A Raman spectroscopic study. Physics and Chemistry of Minerals, 20, 556–562.

Reynard, B., Fiquet, G., Itié, J.-P., and Rubie, D.C. (1996a) High-pressure X-ray diffraction study and equation of state of $MgSiO_3$ ilmenite. American Mineralogist, 81, 45–50.

Reynard, B., Takir, F., Guyot, F., Gwanmesia, G.D., Liebermann, R.C., and Gillet, P. (1996b) High-temperature Raman spectroscopic and X-ray diffraction study of β-Mg_2SiO_4: Insights into its high-temperature thermodynamic properties and the β- to α-phase-transformation mechanism and kinetics. American Mineralogist, 80, 585–594.

Sawamoto, H. (1987) Phase diagram of $MgSiO_3$ at pressures up to 24 GPa and temperatures up to 2200 °C: Phase stability and properties of tetragonal garnet. In M.H. Manghnani and Y. Syono, Eds., High pressure research in mineral physics, p. 209–220. Terrapub AGU, New York.

Tsukimura, K., Sato-Sorensen, Y., Ghose, S., and Sawamoto, H. (1988) High-temperature single-crystal study of β-Mg_2SiO_4. Eos, 69, 498.

Weidner, D.J., and Ito, E. (1985) Elasticity of $MgSiO_3$ in the ilmenite phase. Physics of the Earth and Planetary Interiors, 40, 65–70.

Wolf, G.H., Wang, S., Herbst, C.A., Durben, D.J., Oliver, W.F., Kang, Z.C., and Halvorson, K. (1992) Pressure induced collapse of the tetrahedral framework in crystalline and amorphous GeO_2. In Y. Syono and M.H. Manghnani, Eds., High pressure research: Applications to Earth and planetary sciences, p. 503–517. AGU Terrapub, Washington, DC.

Yamanaka, T. (1986) Crystal structures of Ni_2SiO_4 and Fe_2SiO_4 as a function of temperature and heating duration. Physics and Chemistry of Minerals, 13, 227–232.

Manuscript received June 29, 1995
Manuscript accepted April 30, 1996